Science of the Total Environment 739 (2020) 140343

Contents lists available at ScienceDirect

Science of the Total Environment

journal homepage: www.elsevier.com/locate/scitotenv

Shifts in carbon and nitrogen stable isotope composition and epicuticular lipids in leaves reflect early water-stress in vineyards

Jorge E. Spangenberg [a,*], Marc Schweizer [a], Vivian Zufferey [b]

[a] Institute of Earth Surface Dynamics (IDYST), University of Lausanne, CH-1015 Lausanne, Switzerland
[b] Institute of Plant Production Sciences (IPV), Agroscope, CH-1009 Pully, Switzerland

HIGHLIGHTS

- The potential of leaf composition as early plant water stress marker is explored.
- $\delta^{13}C$ increases with water deficit only in non-organic-fertilized vines.
- $\delta^{15}N$ and N content decrease with water deficit during the growing season.
- Total vine epicuticular fatty acids content increases in response to water deficit.

GRAPHICAL ABSTRACT

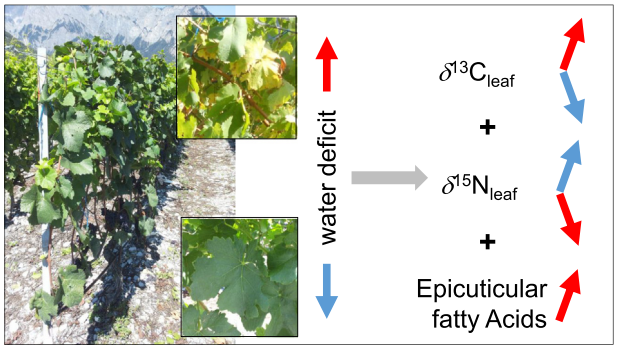

ARTICLE INFO

Article history:
Received 6 May 2020
Received in revised form 12 June 2020
Accepted 16 June 2020
Available online 19 June 2020

Editor: José Virgílio Cruz

Keywords:
Climate change
Compound-specific isotope analysis
$\delta^{13}C$ and $\delta^{15}N$
Fatty acids
Leaf waxes
Linoleic and linolenic acids
Plant water relations
Student's *t*-test
Water stress

ABSTRACT

Changes in leaf carbon and nitrogen isotope composition ($\delta^{13}C$ and $\delta^{15}N$ values) and the accumulation of epicuticular lipids have been associated with plant responses to water stress. We investigated their potential use as indicators of early plant water deficit in two grapevine (*Vitis vinifera* L.) cultivars, Chasselas and Pinot noir, that were field-grown under well-watered and water-deficient conditions. We tested the hypothesis that the bulk $\delta^{13}C$ and $\delta^{15}N$ values and the concentrations of epicuticular fatty acids may change in leaves of similar age with the soil water availability. For this purpose, leaves were sampled at the same position in the canopy at different times (phenological stages) during the 2014 growing season. Bulk dry matter of young leaves from flowering to veraison had higher $\delta^{13}C$ values, higher total nitrogen content, and lower $\delta^{15}N$ values than old leaves. In both cultivars, $\delta^{15}N$ values were strongly correlated with plant water deficiency, demonstrating their integration of the plant water stress response. $\delta^{13}C$ values recorded the water deficiency only in those plants that had not received foliar organic fertilization. The soil water deficiency triggered the accumulation of $C_{>26}$ fatty acids in the cuticular waxes. The compound-specific isotope analysis (CSIA) of fatty acids from old leaves showed an increase in $\delta^{13}C$ among the C_{16}-C_{22} chains, including stress signaling linoleic and linolenic acids. Our results provide evidence for leaf ^{13}C-enrichment, ^{15}N-depletion, and enhanced FA-chain elongation and epicuticular accumulation in the grapevine response to water stress. The leaf $\delta^{13}C$ and $\delta^{15}N$ values, and the concentration of epicuticular fatty acids can be used as reliable and sensitive indicators of plant water deficit even when the level of water stress is low to moderate. They could also be used, particularly the more cost-efficient $\delta^{13}C$ and $\delta^{15}N$ measurements, for periodic biogeochemical mapping of the plant water availability at the vineyard and regional scale.

* Corresponding author.
E-mail address: Jorge.Spangenberg@unil.ch (J.E. Spangenberg).

https://doi.org/10.1016/j.scitotenv.2020.140343
0048-9697/

1. Introduction

Plants respond to the impact of environmental stresses, particularly heat and drought, by changes in photosynthesis and metabolism, which is reflected in the carbon and nitrogen isotope composition ($\delta^{13}C$ and $\delta^{15}N$ values) of tissues and the stoichiometry of primary and secondary metabolites. Grapevine (*Vitis vinifera* L.) is highly sensitive to water deficiency and is also one of the most expensive cultivated crops in the world. In the face of climate change, there is therefore a need to develop markers of early plant water stress to optimize water management and reduce adverse effects on crop yield. In this context, we explored the potential of leaf $\delta^{13}C$ and $\delta^{15}N$ values, and the accumulation of epicuticular lipids as indicators of early plant water deficit.

Variations in the $\delta^{13}C$ values of plant leaves may reveal the response of plants to global and local environmental conditions (Farquhar et al., 1982; Brugnoli et al., 1988; Cernusak et al., 2013). The physiological mechanism underlying leaf ^{13}C enrichment in water-deficient plants is attributed to the downregulation of stomatal conductance (g_s) and increased water use efficiency (WUE) (Farquhar et al., 1982, 1989). This change in leaf ^{13}C discrimination could serve as a time-integrator of WUE (Condon et al., 2004). The $\delta^{15}N$ values of the total nitrogen (TN) in plant tissues are primarily controlled by the isotopic composition of the N sources (soil, precipitation, N_2 fixation, N fertilization), forms (NH_4^+, NO_3^-, organic N) and by how N is taken up—symbiotic association with mycorrhizal fungi and/or N-fixing bacteria (Högberg, 1997; Hobbie et al., 1999). Further discrimination against ^{15}N is associated with transformations during N uptake, translocation, assimilation, and reallocation within a plant and among leaves (Evans, 2001; Werner and Schmidt, 2002). The availability and form of nitrogen are critical for the $\delta^{15}N$ value of the plant organic matter (Evans, 2001; Tcherkez and Hodges, 2008). Both water availability and temperature influence N mineralization, NH_3 volatilization, and denitrification processes, which change the contributions of the forms of N available to the plant, and the difference between plant and soil $\delta^{15}N$ values (Högberg, 1997). Few studies have reported the effects of drought on plant $\delta^{15}N$ (Handley et al., 1999; Robinson et al., 2000; Craine et al., 2015). It was recently shown that ^{13}C and ^{15}N contents in leaves vary with age and plant development (Liu et al., 2019; Werth et al., 2015). Therefore, a study of the changes in leaf $\delta^{13}C$ and $\delta^{15}N$ values in response to water stress should include leaves during different stages (i.e., phenological stages) of plant growth under different soil-water regimes.

The outermost layer of leaves is composed of hydrophobic compounds, i.e., epicuticular waxes, which have as essential function the protection of leaves from uncontrolled water loss during their development (Kerstiens, 1996; Jetter et al., 2000; Dominguez et al., 2017). Epicuticular waxes are a mixture of long-chain compounds, including *n*-alkanoic acids (fatty acids, FAs), *n*-alkanols, *n*-aldehydes, and *n*-alkanes, derived from FAs of 16 to 34 carbons (C_{16}–C_{34}) (Jetter et al., 2000). These compounds are formed in the endoplasmic reticulum of epidermal cells and exported to the environmental surface of the leaf epidermis (Bernard and Joubes, 2013). Leaf lipids and fatty acids show persistent changes during periods of drought and/or heat, which is not the case for other compounds, such as soluble sugars and amino acids, which change only periodically (Impa et al., 2020; Zinta et al., 2018). Concentrations and compound-specific carbon isotope analysis (CSIA, $\delta^{13}C$) of epicuticular wax FAs, *n*-alkanes, and *n*-alkanols were used to obtain information about plant-ecosystem interactions in modern and past environments (Srivastava and Wiesenberg, 2018; Wang et al., 2018; Wu et al., 2017). To our knowledge, no studies have addressed the effect of leaf age and plant water availability on the abundance and $\delta^{13}C$ of epicuticular fatty acids.

Recently, using three grapevine cultivars (Chasselas, Petite Arvine and Pinot noir) and six growing seasons (2009–2014), we have shown that the $\delta^{13}C$ values of grape sugars at harvest are highly correlated with the predawn leaf water potential (Ψ_{pd}) (Spangenberg et al., 2017; Spangenberg and Zufferey, 2018). This relationship was preserved in the derived whole wines, as well as in the wine ethanol, wine main volatile compounds, and solid residues obtained by freeze-drying wine aliquots (Spangenberg et al., 2017; Spangenberg and Zufferey, 2018, 2019). The main outcome of these studies was that the $\delta^{13}C$ of these wine components could be used to study the evolution of soil water status in vineyard regions. Additionally, the C/N molar ratios and $\delta^{15}N$ of the wine solid residues were also highly correlated with Ψ_{pd} for Chasselas and Pinot noir vines, and could also serve as indicators of soil water status and nitrogen dynamics in the soil-water-plant system (Spangenberg et al., 2017; Spangenberg and Zufferey, 2018).

The present study aimed to test whether leaf $\delta^{13}C$ and $\delta^{15}N$ values and the composition of epicuticular FAs could serve as early indicators of water deficiency in grapevines. Thus, the response of these parameters to plant water deficit was assessed in leaves of different age and plant development stage. The studied leaves were from 2014 experiments with the white wine cultivar Chasselas and red wine cultivar Pinot noir, both growing under the same environmental and climatic conditions and differing only in soil water status through controlled irrigation treatments. The goal of this experiment was to determine whether the effects of water deficit could be measured in the leaf $\delta^{13}C$ and $\delta^{15}N$ values and the wax FA concentrations at different stages of leaf and plant development. In particular, the objectives were to (i) determine responses of leaf $\delta^{13}C$ and $\delta^{15}N$ values and wax FA concentrations to water deficit at different times during the growing season; (ii) establish if these trends are similar between cultivars and how they relate to Ψ_{pd} and leaf gas exchange parameters; (iii) establish if water deficit affects the distribution and $\delta^{13}C$ values of wax FAs; and (iv) provide mechanistic insights into the effect of water deficiency on foliar $\delta^{13}C$ and $\delta^{15}N$ and epicuticular fatty acids. The overall motivation of our experiment was to provide information concerning the evolution of leaf $\delta^{13}C$ and $\delta^{15}N$ and surface wax lipids in plants growing under different water availabilities and test their potential as biochemical tools to monitor plant water stress at the regional scale.

2. Materials and methods

2.1. Plant material, growth conditions and irrigation experiment

The irrigation experiments were performed on field-grown Chasselas and Pinot noir grapevines during the 2014 growing season at the experimental station of Agroscope at Leytron (46°11′N; 7°12′E) in Valais, Switzerland. The vineyards are located in an alpine valley filled with torrential alluvial deposits; the soils are >2.5 m deep and sandy to very stony, with a uniform water holding capacity of 150 mm at the vineyard scale (Zufferey et al., 2017, 2018). The climate at Leytron is relatively dry, generally warm, and temperate, with a significant amount of rainfall throughout the year. During 2014, the monthly mean precipitation from bud (May/June) to grape maturation/harvest (September) was between 15 and 106 mm, and the monthly mean temperature was between 15.6 and 20.1 °C—up to 2 °C higher than the 1981–2010 average values (see Supporting Information Table S1). The weather conditions during grape development were typical of a hot and rainy summer. The atmospheric CO_2 concentration was monitored during the trial and remained constant over the past ten years at 390 ppmv in daylight and 10 ppmv higher in darkness due to plant and soil respiration.

The white cv. Chasselas (clone 14/33-4) and the red cv. Pinot noir (clone 9–18) were grafted onto *Vitis berlandier* x *Vitis riparia* cv. Kober-5BB rootstock. Both cultivars were grown under the same natural field conditions. All the vine plants were 20 years old at the time of leaf sampling. Only the Chasselas vines had an addition of foliar urea, 5 kg N ha^{-1} once a week for four weeks during veraison, between days of the year (DOY) 220 and 240. The irrigation experiment was performed using 40 plants per treatment in a randomized block design of 10 vines per block (Zufferey et al., 2018). Different soil water status conditions were established, from well-watered to water deficit conditions,

using three different irrigation treatments: drip irrigation (DI) with a weekly feed of 9 L m^{-2} of soil (16 L $vine^{-1}$) from bloom (DOY ~ 150) to fruit ripening (DOY ~ 215), no irrigation (NI) with rain-fed plants, and no irrigation and soil covered with a waterproof and nonreflecting plastic (NIP) to prevent the infiltration of precipitation water during the growing season.

2.2. Plant water status and leaf gas exchange measurements

The plant water status was assessed through measurement of the predawn leaf water potential (Ψ_{pd}, MPa) from bloom to harvest (July to September) using a pressure chamber (model 3005; Soil Moisture Equipment Corp., Santa Barbara, CA, USA). The Ψ_{pd} measurements were performed weekly in fully expanded and well-exposed leaves in the median part of the shoot in complete darkness between 0400 and 0500 h. The reported Ψ_{pd} values are the mean ± 1 standard error (SE) of four to six measurements. Grapevine is highly water-stressed under Ψ_{pd} values lower than −0.5 MPa; under values between −0.5 and −0.3 MPa, the water deficit is moderate; under values higher than −0.3 MPa, the plant is considered to be under low or no water stress (van Leeuwen et al., 2009).

The leaf gas exchange parameters were determined nondestructively for healthy, fully expanded, mature, and non-senescent median leaves that were well exposed to direct sunlight (photon flux density PFD > 1800 μmol m^{-2} s^{-1}). Measurements of the net photosynthetic rate (A, μmol CO_2 m^{-2} s^{-1}), transpiration rate (E, mmol H_2O m^{-2} s^{-1}), stomatal conductance (g_s, mmol CO_2 m^{-2} s^{-1}) and mesophyll resistance (r_m, bar mol^{-1}) were performed for eight leaves per treatment in the mid-morning (1000 h local time) on clear-sky days using a portable gas-exchange system (LI-6400, LI-COR Inc., Lincoln, NE, USA). The r_m was calculated as $r_m = (C_i - \Gamma)/A$, where C_i is the intercellular partial pressure of CO_2 and Γ is the CO_2 compensation point (Schultz et al., 1996). The A and g_s values were used to calculate the intrinsic WUE ($WUE_i = A/g_s$, μmol CO_2 $mmol\ H_2O^{-1}$). Leaf temperature was measured with a thermistor incorporated in a leaf LI-COR chamber analyzer.

2.3. Samples

Leaf samples were collected from 1000 to 1500 h on sunny days from three to six randomly chosen plants per genotype (Chasselas, Pinot noir) at different stages of leaf and plant development and with different soil water availabilities. Four to eight leaves were collected at different positions in the canopy, i.e., basal (old), median, and apical (young), in replicate plants under different water treatments (DI, NI, NIP) during four phenological stages, including flowering (DOY 171), pea-sized stage (DOY 206), veraison (DOY 222), and harvest (DOY 269). The intertreatment variations in the leaf total organic carbon (TOC), TN, $\delta^{13}C$, and $\delta^{15}N$ values were studied in composite samples of four leaves collected from the median part of different shoots per plant. The composite samples were replicated for three plants selected at random within each irrigation treatment block. Only primary leaves that were fully expanded and undamaged, showing no signs of alteration or surface debris, were sampled. Leaves were collected by cutting the base of the petiole using a scalpel and forceps. The leaves were carefully washed with deionized water (DIW) to remove dust and adhering materials with help of preheated (500 °C, 4 h) quartz wool, rinsed with Milli-Q water (MQW, DIW purified with a Direct-Q UV 3 Millipore® System, Merck, Darmstadt, Germany), carefully stretched horizontally on preheated aluminum foil, wrapped around, placed in a labeled plastic bag and stored in a chilled icebox before being transported to the UNIL-IDYST laboratories, where they were stored at −20 °C until analysis. The area of the leaves collected for FA analysis was determined following Carbonneau (1976). Soil samples were collected at the sites of the experiments (Chasselas and Pinot noir blocks, with DI, NI, and NIP treatments) in duplicate and at two depth intervals (0.5–30 cm, 30–60 cm) to determine the TN content and $\delta^{15}N$ value of the soil nitrogen source to the vines. The description of the soil sample preparation, analysis and results, including pH, TOC, TN, $\delta^{13}C_{TOC}$ and $\delta^{15}N_{TN}$ can be found in the Supporting Information, Table S2.

2.4. Sample preparation

For stable isotope analysis, the leaves were cut into small pieces with solvent-cleaned scissors, freeze-dried on a Lyovac GT2 lyophilizer (SRK Systemtechnik GmbH, Goddelau, Germany), powdered under liquid nitrogen, and stored in borosilicate vials at −20 °C before analysis.

The powders of four leaves per shoot position or per plant were combined and homogenized to produce the composite samples for intraplant and intertreatment comparisons. For FA analysis, the leaves were kept at −20 °C before surface lipid extraction, which was generally performed within 48 h after collection. All the material and glassware used for sample handling and lipid extraction were thoroughly washed, rinsed with DIW and MQW, and heated (480 °C, >4 h) before use.

2.5. Bulk stable carbon and nitrogen isotope analysis

The TOC, TN, $\delta^{13}C$, and $\delta^{15}N$ values of the median leaf samples were determined by elemental analysis/isotope ratio mass spectrometry (EA/IRMS) using a Carlo Erba 1108 (Fisons Instruments, Milan, Italy) elemental analyzer connected to a Delta V Plus isotope ratio mass spectrometer via a ConFlo III interface (both of Thermo Fisher Scientific, Bremen, Germany). For the $\delta^{13}C$ and $\delta^{15}N$ analyses, separate EA combustions were performed using sample aliquots with a 1:50 weight-size difference. The stable isotope compositions were reported in the delta (δ) notation as variations of the molar ratio (R) of the heavy (^iE) to light (^jE) isotope of element E ($^{13}C/^{12}C$ and $^{15}N/^{14}N$) relative to an international standard (Coplen, 2011):

$$\delta^i E_{sample/standard} = \frac{R\left({}^iE/{}^jE\right)_{sample}}{R\left({}^iE/{}^jE\right)_{standard}} - 1$$

For $\delta^{13}C$, the standard is Vienna Pee Dee Belemnite limestone (VPDB); for $\delta^{15}N$, the standard is air molecular nitrogen (Air-N_2). The unit of the δ-values is the urey (Ur), according to the guidelines of the International Union of Pure and Applied Chemistry (IUPAC) (Brand, 2011). One milliurey (mUr) equals 1 per mil (‰), which is not a IUPAC unit; it is deprecated but still used for δ-values. For calibration and normalization of the measured δ-values, a 3- or 4-point calibration was used with international and in-house standards (Spangenberg and Zufferey, 2019). The repeatability and intermediate precision of the EA/IRMS analyses were determined by the standard deviation (SD) of separately replicated analyses ($n \geq 3$) and were better than 0.05 and 0.1 mUr for $\delta^{13}C$ and $\delta^{15}N$, respectively. The accuracy of the analyses was checked periodically with RMs. The carbon and nitrogen concentrations were determined from the peak areas of the major isotopes using the calibrations for $\delta^{13}C_{VPDB}$ and $\delta^{15}N_{Air\text{-}N2}$ and they showed a repeatability better than 0.1 wt% for TOC and TN contents.

2.6. Extraction of epicuticular lipids, total fatty acid separation and methylation

The epicuticular lipids were extracted using a modified procedure from Spangenberg et al. (2014). Individual frozen leaves were thawed rapidly with MQW at 40 °C for 2 min, rinsed with MQW, vacuum-dried, transferred to a beaker, and an aliquot of an internal standard (IS) solution of deuterated carboxylic acids (lauric acid, $C_{12:0}D_{23}$, and arachidic acid, $C_{20:0}D_{39}$; from Cambridge Isotopes Laboratories, CIL, Tewksbury, MA, USA) was added for quantification of the FAs. The surface lipids were extracted by immersion in organic solvent mixtures ($MeOH/CH_2Cl_2$, 1:0, 1:1, and 0:1, each for 30 s). The extracts were

combined, and the excess solvents were removed with a N_2 stream before alkaline hydrolysis (1 M KOH/MeOH, 16 h at room temperature). The FAs were separated with hexane and derivatized (14% BF_3–methanol, 8 min at 60 °C). The formed FA methyl esters (FAMEs) were extracted with hexane, washed with organic solvent-extracted MQW, and stored at −20 °C before analysis.

2.7. Fatty acid identification and quantification

The FAs were analyzed by gas chromatography/mass spectrometry (GC/MS) using an Agilent (Palo Alto, USA) 6890 gas chromatograph connected to a 5973 mass-selective detector (70 eV, source 230 °C, quadrupole 150 °C) in multiple-ion detection mode over m/z 20 to 550. Helium was the carrier gas (1.2 mL/min). The FAMEs were separated with a HP-ULTRA 2 fused-silica column (50 m × 0.32 mm i.d. coated with 0.17 μm 5% phenylmethylsilicone). Samples were injected splitless at 320 °C. After an initial period of 2 min at 100 °C, the column was heated to 310 °C (held 20 min) at 4 °C/min. Compound assignment was based on comparison with standard mass spectra in the NIST14 Mass Spectral Library (National Institute of Standards and Technology, MD, USA), GC retention time, and MS fragmentation patterns. Concentrations of FAs were determined by GC/flame ionization detection (GC/FID) using a 7890B gas chromatograph (Agilent Technologies, Wilmington, DE, USA) equipped with a 7693A autosampler and a flame ionization detector. The column and chromatographic conditions were the same as those used for GC/MS. Quantitative FA data were obtained from the GC/FID peak area ratios of unknown and IS of known concentration, and expressed as μg per unit leaf area (μg cm^{-2}).

2.8. Carbon isotope analysis of individual fatty acids

The compound-specific isotope analysis (CSIA) of the FAMEs ($\delta^{13}C_{FAME}$) was performed by GC/combustion/isotope ratio MS (GC/C/IRMS) using an Agilent 6890 GC instrument connected to a Delta V Plus isotope ratio mass spectrometer via a combustion interface III (both from Thermo Fisher Scientific, Bremen, Germany). GC separation was performed with the same column and temperature program used for GC/MS and GC/FID. The known $\delta^{13}C$ values (determined by EA/IRMS) of the deuterated carboxylic acids added as IS were used for calibration and standardization of the GC/C/IRMS measurements. The repeatability and intermediate precision of the GC/C/IRMS analysis and the performance of the GC and combustion interface were evaluated by regular injection of the methyl-eicosanoate standards USGS70 ($\delta^{13}C$: −30.43 mUr), USGS71 ($\delta^{13}C$: −10.50 mUr), and USG72 ($\delta^{13}C$: −1.54 mUr) (Schimmelmann et al., 2016) and replicate ($n = 3$–6) analyses of the FAME fractions of leaf epicuticular lipids. The standard deviation for repeatability of the $\delta^{13}C_{FAME}$ values depended on the concentration of the FAMES, varying between ±0.05 and ± 0.5 mUr (for m/z 45 peak sizes between 15,000 mV and 500 mV, respectively). The $\delta^{13}C$ value of FA ($\delta^{13}C_{FA}$) was obtained by correcting the $\delta^{13}C_{FAME}$ for the isotopic shift due to the carbon introduced by methylation.

2.9. Statistical analysis and data presentation

Data were statistically analyzed using the SPSS software package V25.0 (SPSS Inc., Chicago, IL, USA). All values reported are the mean ± SE for four to eight biologically independent replicates. Data were tested for homogeneity of variance with the F-test, and the means of each treatment group were compared using the paired-samples Student's t-test. The significance level for all tests was set at $P < 0.05$. A bivariate correlation procedure was used to calculate the Pearson correlation coefficients and linear regression equations. Figures were prepared using DeltaGraph V6.0.21 (Red Rock Software Inc., UT, USA) and Adobe Illustrator 2020 V24.0.3 (Adobe Systems Inc., CA, USA).

3. Results

3.1. Leaf water status and gas exchange

For both cultivars, no signs of senescence were observed in old basal leaves at the onset of the water-deficit treatments, or in well-watered plants throughout the experiment. The leaf temperature ranged from 24.0 to 28.5 °C, corresponding to the optimal temperature for maximum photosynthesis (Zufferey et al., 2000). There were no differences in leaf temperatures between well-watered and water-deficient vines (Table S3). During the grape ripening period from veraison until harvest, DOY 233–269, the Ψ_{pd}, g_s, E, and A were lower ($P < 0.05$) for both cultivars in water-deficient than well-watered plants (Fig. 1). The decrease in g_s and A was observed at the same time and in a proportional manner when the water stress gradually increased during the growing season. The lowestΨ_{pd} values (−0.3) were measured in the water-deficient (NIP) vines during the onset of fruit-ripening, with the lowest g_s, E, and A in NIP plants at harvest. Conversely, the r_m increased during the season (from flowering to harvest) as well as with water constraint (between DI and NIP plants) (Table S3). Furthermore, the differences in the Ψ_{pd} values at harvest between well-watered and water-deficient regimes were similarly small for both cultivars ($\Delta\Psi_{pd\text{-}NIP/DI} = \Psi_{pd\text{-}NIP} - \Psi_{pd\text{-}DI} = -0.18$ and −0.16 MPa for Chasselas and Pinot noir, respectively) and associated with a small decrease in g_s ($\Delta g_{s\text{-}NIP/DI} = g_{s\text{-}NIP} - g_{s\text{-}DI} = -65$ an −85 mmol CO_2 m^{-2} s^{-1}), E ($\Delta E_{\text{-}NIP/DI} = E_{NIP} - E_{DI} = -0.7$ and −1.0 mmol H_2O m^{-2} s^{-1}), A ($\Delta A_{\text{-}NIP/DI} = A_{NIP} - A_{DI} = -3.0$ and −3.3 mmol CO_2 m^{-2} s^{-1}), and WUE_i (A/g_s; $\Delta WUE_{i\text{-}NIP/DI} = WUE_{i\text{-}NIP} - WUE_{i\text{-}DI} = -0.001$ and 0.001 μmol CO_2 mmol H_2O^{-1}) (Table S3). These differences indicate that the irrigation treatments imposed a low to moderate water deficit, which did not induce a significant stomatal closure and increase in leaf temperature.

3.2. Variations in leaf $\delta^{13}C$, TN and $\delta^{15}N$ values

Important variations were observed in the $\delta^{13}C$, TN, and $\delta^{15}N$ values during the growing season (Fig. 2 and Table S4). The patterns of the foliar $\delta^{13}C$ values differed significantly between the cultivars. For Pinot noir, the variations followed an expected trend during the growing season, with significantly lower $\delta^{13}C$ values in well-watered plants and higher values in water-deficient plants. Under all water treatments, the $\delta^{13}C$ values decreased from flowering to veraison (DOY 171–233), and at harvest increased by up to 1.5 mUr compared with veraison. This ^{13}C enrichment independent of the soil water availability was most probably due to the reallocation of organic compounds during leaf senescence (see Section 4.1.). The greatest change in ^{13}C values with increasing water deficiency ($\Delta^{13}C_{NIP/DI} = \delta^{13}C_{NIP} - \delta^{13}C_{DI}$) was observed at flowering (1.98 mUr), and the smallest changes were observed at harvest (0.83 mUr). For Chasselas, the $\delta^{13}C$ values showed a $\delta^{13}C_{DI} \approx \delta^{13}C_{NIP} < \delta^{13}C_{NI}$ trend at flowering and the pea-sized berry stage and a change in the opposite direction ($\delta^{13}C_{NI} < \delta^{13}C_{NIP} \approx \delta^{13}C_{DI}$) at veraison and harvest (Fig. 2a). This inversion of the $\delta^{13}C$ trend together with more significant differences (up to 2.3 mUr, $P < 0.01$) between the irrigation treatments occurred after foliar application of urea. In fact, the absorption of urea-N from fertilizer —which had a $\delta^{13}C$ value of −40.01 ± 0.03 mUr and $\delta^{15}N$ of −2.35 ± 0.09 mUr (Table S2)—added ^{13}C-depleted carbon to the leaves. At harvest, the $\delta^{13}C$ differences between the water treatments were smaller, probably due to a dilution of the ^{13}C-depleted compounds through the assimilation of new carbon.

The TN content was on average similar for both cultivars (2.46 ± 0.11 wt% for Chasselas, 2.62 ± 0.21 wt% for Pinot noir) despite the foliar urea application to Chasselas vines, and it decreased throughout the growing season (up to 0.76 wt% for Chasselas, 1.59 wt% for Pinot noir) (Fig. 2b,e). Generally, from flowering onwards, the TN content decreased with soil water availability. The $\delta^{15}N$ values in Chasselas leaves ranged from 0.54 to 3.38 mUr (1.53 ± 0.38 mUr) and in Pinot noir

leaves from 0.49 to 3.55 mUr (1.92 ± 0.44 mUr). The $\delta^{15}N$ values increased by 3 mUr from flowering to harvest in both cultivars, as best evidenced in well-watered vines (Fig. 2c,f). The only source of N for Pinot noir vines was the soil TN (i.e., NH_4^+, NO_3^-, and organic N), the $\delta^{15}N$ values of which could be expected to be ≥4.0 mUr, sourced from soil TN, which had an average $\delta^{15}N$ of 4.06 ± 0.19 mUr (Table S2). Therefore, on average, the vine leaves discriminated against ^{15}N by 2.0 mUr ($\Delta^{15}N_{Source/Leaf} = \delta^{15}N_{Sourve} - \delta^{15}N_{Leaf}$). Specifically, the $\delta^{15}N$ values changed significantly ($P < 0.05$) after flowering under water deficiency, with lower $\delta^{15}N$ values—up to 2 mUr in Chasselas and 3 mUr in Pinot noir leaves— in water-deficient than in well-watered plants. Notably, in Chasselas vines, the addition of foliar urea-N (during DOY 220–240) had no distinct effect on either leaf TN or $\delta^{15}N$ values, it was best observed in the leaves of well-watered vines.

3.3. Variation in the fatty acid composition of epicuticular lipids

The FAs in epicuticular lipids of leaves from both cultivars were straight-chain carboxylic acids with an even-over-odd predominance in the C_{14}–C_{32} range and peaked on average at C_{24} (see Supplementary Information, Fig. S1 and Table S5). The FAs are abbreviated as C*x*:*y*, where '*x*' is the number of carbons and '*y*' is the number of double bonds. For both cultivars, the very long chain FAs (VLCFAs) with $C_{>18}$ saturated structures occurred in a significantly higher proportion than short-chain homologs. The main saturated acids were palmitic ($C_{16:0}$), stearic ($C_{18:0}$), arachidic (eicosanoic acid, $C_{20:0}$), docosanoic ($C_{22:0}$), tetracosanoic ($C_{24:0}$), pentacosanoic ($C_{25:0}$), hexacosanoic ($C_{26:0}$), octacosanoic ($C_{28:0}$), triacontanoic ($C_{30:0}$), and dotriacontanoic ($C_{32:0}$) acids. The monounsaturated FAs ($C_{16:1}$, $C_{18:1}$) were either not detected or present only in trace amounts (Fig. S1). The only polyunsaturated FAs (PUFAs) that were identified and quantified were linoleic ($C_{18:2}$) and linolenic ($C_{18:3}$) acids. The total FA (TFA) contents per unit leaf area (μg cm^{-2}) were calculated by adding the 13 FAs quantified in all leaves, which varied between 0.31 and 11.89 μg cm^{-2} and were slightly higher (not significant for $P < 0.05$) in Pinot noir leaves (4.15 ± 1.85 μg cm^{-2}, $n = 60$) than Chasselas leaves (3.00 ± 3.30 μg cm^{-2}, $n = 60$) (Tables S5 and S6).

For the study of intraplant variation in the accumulation of epicuticular lipids, leaf surface lipids were extracted from four basal and three apical leaves per plant and replicated for three randomly chosen plants in the experimental blocks (Fig. 3 and Table S5). At flowering, the apical leaves in rain-fed vines of both cultivars had a slightly higher TFA content (not significant for $P < 0.05$) than basal leaves. At harvest, independent of the water treatment, the basal leaves had significantly higher TFAs than apical leaves, except for the well-watered Pinot noir vines, in which the basal leaves were relatively depleted of surface lipids. Clearly, water deficiency increased the epicuticular TFAs. The response of the TFA content of median leaves to soil water availability during the growing season is shown in Fig. 4. The TFA contents steadily increased from flowering to harvest for both cultivars and were significantly higher in water-deficient than well-watered plants. Interestingly, the slope of the TFA vs. DOY regression line—which estimates the rate of deposition of epicuticular waxes in the median leaves—was similar for well-watered plants of both cultivars. For Chasselas vines, the slope did not change significantly with water deficiency. However, for Pinot noir, the slope of the TFA-DOY line was greater for the water-deficient vines than well-watered plants, as well as for the water-deficient Chasselas vines (Fig. 4).

Further differences between cultivars, plant developmental stage, leaf age, and soil water availability were mainly related to the relative abundance of FAs. At flowering (DOY 171), the most abundant FAs on basal leaves from rain-fed vines of both cultivars were C_{24}, C_{26}, and C_{28} (Fig. 5). The apical leaves contained a significantly higher relative abundance of C_{16} and C_{18} FAs—74.3 and 80% of the TFA for Chasselas and Pinot noir, respectively—than basal leaves. This difference was more pronounced for $C_{18:2}$ and $C_{18:3}$, which composed 55.9 and 54.3% of the TFA in the apical leaves of Chasselas and Pinot noir, respectively. At harvest (DOY 269), long-chain C_{20}–C_{32} FAs occurred in the basal and apical leaves from both cultivars in significantly higher amounts (up to 78.3% of the TFA) than the short- and mid-chain C_{16}–C_{18} homologs (Fig. 6). The increase in the relative abundance of the C_{20}–C_{32} FAs with plant development and leaf age was accompanied by a decrease in the content of C_{16}–C_{18} saturated FAs, which was more pronounced in $C_{18:2}$ and $C_{18:3}$ (Figs. 5 and 6). For both cultivars, the only significant difference between well-watered and water-deficient plants was the higher relative abundance of C_{28}–C_{32} FAs in both basal and apical leaves (Fig. 6).

3.4. Carbon isotope composition of the individual fatty acids

The response of the plants to low soil water availability by synthesizing more epicuticular lipids was studied further by compound-specific carbon isotope analysis of FAs ($\delta^{13}C_{FA}$ values) in basal and apical leaves at harvest (Fig. 7). The $\delta^{13}C$ values of the C_{16}–C_{32} FAs for both cultivars under different water treatments varied from −39.6 to −30.9 mUr. In all leaves, the $C_{16:0}$ and $C_{18:0}$ FAs were enriched in ^{13}C, typically by 1–2 mUr compared with $C_{\geq 20}$ FAs. The difference between $\delta^{13}C_{18:0}$ and $\delta^{13}C_{18:2}$ values ($\Delta^{13}C_{18:0-18:2} = \delta^{13}C_{18:0} - \delta^{13}C_{18:2}$) ranged from 2.2 to 6.8 mUr and was smaller for $\Delta^{13}C_{18:2-18:3}$ ($\Delta^{13}C_{18:2-18:3} = \delta^{13}C_{18:2} - \delta^{13}C_{18:3}$ ranging from −2.6 to −0.1 mUr). In Chasselas vines that received foliar ^{13}C-depleted urea, both basal and apical leaves showed similar $\delta^{13}C_{FA}$ patterns under the different water treatments and only significantly lower $\delta^{13}C$ values in $C_{18:2}$ of water-deficient plants (Fig. 7a,b). Water deficiency also induced a ^{13}C enrichment in C_{24}–C_{32} VLCFAs, but it was only significant at $P < 0.05$ for $C_{26:0}$. In Pinot noir basal leaves, the $\delta^{13}C$ values of the C_{18}-C_{22} FAs increased significantly with water stress, demonstrating the largest difference (7.6 mUr) in $C_{20:0}$ (Fig. 7c,d).

4. Discussion

4.1. Changes in leaf carbon isotope discrimination with water availability

The changes in discrimination against ^{13}C in leaves during the growing season may reflect variations in the contribution of carbon translocated from older to younger leaves and the carbon supplied by its own assimilates. The ^{13}C enrichment in Pinot noir median leaves at harvest, independent of water availability, may be explained by the degradation of the photosynthetic system during leaf senescence. The less effective CO_2 assimilation, carbon fixation, and respiration in old and damaged photosynthetic tissues within old leaves led to a ^{13}C enrichment of photosynthates and synthesized compounds (e.g., Jefferies and MacKerron, 1997; Kitajima et al., 2002).

The C_3 plants exposed to drought and therefore to a restricted stomatal conductance will favor a ^{13}C enrichment of the photosynthate (carbohydrates) and synthesized products (e.g., Farquhar et al., 1989; Flexas and Medrano, 2002). For both Chasselas and Pinot noir vines, water deficiency during the growing season induced some stomatal closure, as shown by the decrease in leaf conductance, photosynthetic rate, and evapotranspiration rate, and an increase in mesophyll resistance (Table S3). For Pinot noir, the leaf $\delta^{13}C$ values increased in response to water deficiency throughout the growing season, which is in agreement with previous studies reporting ^{13}C enrichment in leaves from water-deficient vines (Farquhar et al., 1982; de Souza et al., 2005). In grapevines, the $\delta^{13}C$ values of the sugars ($\delta^{13}C_{sugars}$) accumulated in berries are an integrated measure of the photosynthetic carbon isotope discrimination during fruit ripening and are therefore highly correlated with plant water status (i.e., Ψ_{pd}) (Gaudillère et al., 2002). The berry sugars at harvest from Chasselas and Pinot noir vines from the different experimental blocks had $\delta^{13}C_{sugars}$ values between −27.26 and −26.47 mUr (Spangenberg et al., 2017; Spangenberg and Zufferey, 2018, presented in Table S3). The difference between the $\delta^{13}C_{sugars}$ values for

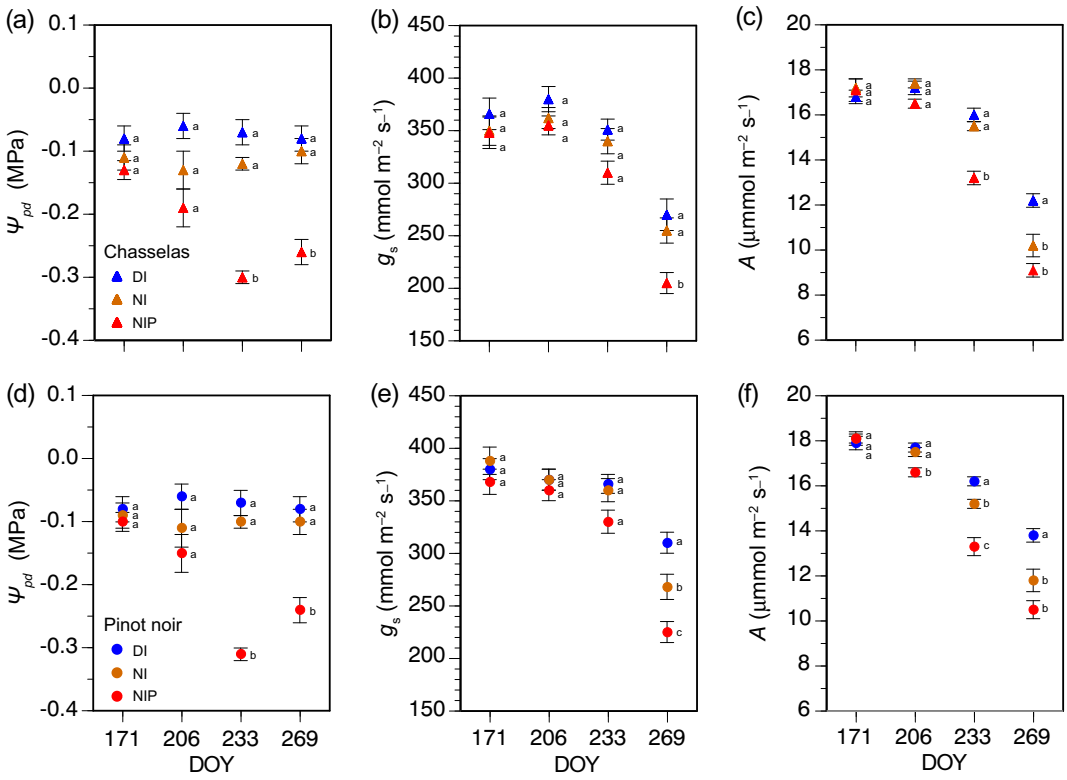

Fig. 1. Changes in water status, gas exchange and photosynthesis in grapevine leaves during growth under different water treatments. Upper plots for Chasselas vines, lower plots for Pinot noir. Data for four phenological stages: flowering (DOY 171), pea-sized berries (DOY 206), veraison (DOY 233), and harvest (DOY 269). (a) and (d) Predawn leaf water potential (Ψ_{pd}); (b) and (e) stomatal conductance (g_s); (c) and (f) net photosynthetic rate (A). The error bars represent the standard error (SE) of the mean from four to six replicates. Symbols marked with different letters indicate a significant difference at $P < 0.05$ based on the Student's t-test. DI: drip irrigation; NI: no irrigation; NIP: no irrigation and plastic-covered soil.

well-watered and water-deficient Pinot noir vines ($\Delta^{13}C_{sugars\text{-}NIP/DI} = \delta^{13}C_{sugars\text{-}NIP} - \delta^{13}C_{sugars\text{-}DI}$) was 0.51 mUr. This $\Delta^{13}C_{sugars\text{-}NIP/DI}$ value corresponded to differences in leaf $\delta^{13}C$ values ($\Delta^{13}C_{leaf\text{-}NIP/DI} = \delta^{13}C_{leaf\text{-}NIP} - \delta^{13}C_{leaf\text{-}DI}$) between 1.98 mUr at flowering and 0.83 mUr at harvest (Fig. 2), which indicated that the response of the leaf $\delta^{13}C$ values to water deficit was amplified by two to four times compared with the $\delta^{13}C_{sugars}$ values. Finally, the application of the foliar urea to Chasselas vines distorted the leaf $\delta^{13}C$ values; therefore, the $\Delta^{13}C_{leaf\text{-}NIP/DI}$ values (−1.45 to 0.15 mUr) could not be compared with $\Delta^{13}C_{sugars\text{-}NIP/DI}$. For both cultivars, there were no significant correlations (Pearson correlation coefficients, r) between the leaf $\delta^{13}C$ and Ψ_{pd}; however, for Chasselas, the ^{13}C was correlated ($P < 0.05$) with *WUE*i (Tables 1 and 2). The nonsignificant $\delta^{13}C$–Ψ_{pd} correlation for both cultivars can be explained by the small Ψ_{pd} range measured during the hot and rainy 2014 growing season (see Table S3). A very weak or no correlation between *WUE*i and leaf $\delta^{13}C$ has been reported for grapevines grown under different irrigation regimes (Bchir et al., 2016; Chaves et al., 2007; de Souza et al., 2005). Therefore, in summary, our results show that leaf $\delta^{13}C$ values can be a reliable and sensitive indicator of time-integrated water deficit in grapevines that have not received any no-atmospheric CO_2 carbon supply (i.e., urea-fertilizer).

4.2. Changes in leaf nitrogen isotope discrimination with water availability

Water deficit substantially affects all aspects of nitrogen assimilation (Lawlor and Cornic, 2002; Tegeder and Masclaux-Daubresse, 2018), including stomatal conductance, different nitrogen sources (i.e., NO_3^-, NH_4^+), leaf N concentration, and activity of N-assimilating enzymes, which may involve discrimination against ^{15}N. We show that for the same phenological stage and age (senescence stage), water deficiency decreased TN and $\delta^{15}N$ values in leaves during the growing season (Figs. 2 and 3). Nitrogen content was strongly positively correlated with the photosynthetic assimilation rate, stomatal conductance (both $P < 0.05$), and transpiration rate ($P < 0.01$) (Tables 1 and 2). Dry soil conditions limit the concentration of water-extractable soil N (i.e., NO_3^- or NH_4^+) in the rhizosphere, the transport of N from the root, and the N distribution to leaves via the transpiration stream (Evans, 2001; Högberg, 1997; Keller, 2005), thereby critically reducing nitrogen availability for assimilation. Therefore, water stress or combined water salinity stress induce a significant decrease in leaf TN and, less importantly, $\delta^{15}N$ values, as shown for plants grown in hydroponic systems (e.g., wild barley, Robinson et al., 2000; durum wheat, Yousfi et al., 2009, 2012; and sweet pepper, Serret et al., 2018). The mechanisms underlying the decrease in TN content and $\delta^{15}N$ values in leaves to water stress response should involve the loss of ^{15}N-enriched compounds. Since water stress induced a decrease in g_s and leaf TN, changes in leaf $\delta^{15}N$ values might be a consequence of changes in the relative importance of internal nitrogen re-assimilatory and transport processes, rather than externally mediated soil processes (Stock and Evans, 2006). The organic nitrogen mobilization during water stress is mainly exercised by autophagy and vacuolar proteolysis (Guiboileau et al. 2013; Tegeder and Masclaux-Daubresse 2018). The emerging free amino acids from protein hydrolysis move to different plant tissues, resulting in different N isotope fractionations (Peuke et al. 2013). It is known that the concentration of free amino acids increases markedly in response to water stress in both leaves and roots, and that in the leaves is dominated by proline (Chaves et al. 2003; Mundim and Pringle 2018; Zinta et al., 2018). Significantly elevated levels of proline were found in response to drought in grapevine leaves (Haider et al. 2017), grape skins (Hochberg et al. 2015), and whole grapes (Canoura et al. 2018). The accumulation of proline in maturing grapes was not associated with an increased level of pyroline-5-carboxylate synthetase, suggesting a dominant contribution from other organs, i.e. leaves (Stines et al. 1999). Proline is ^{15}N enriched compared with other amino acids

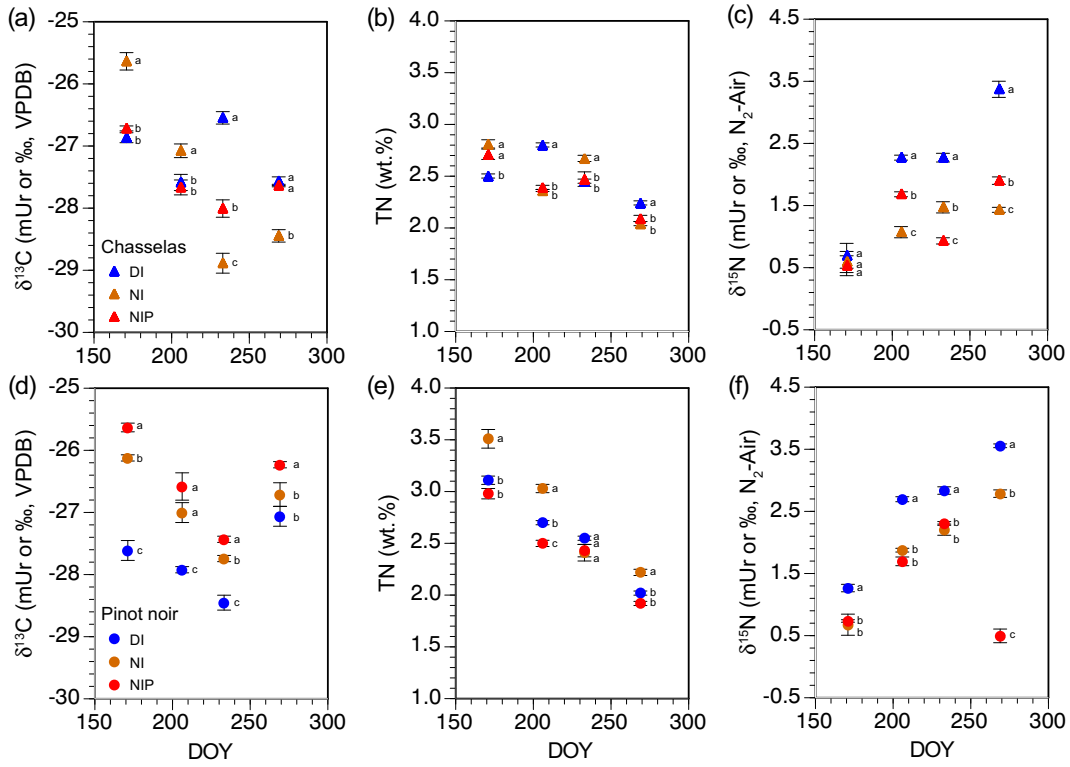

Fig. 2. Effects of water treatment and growing stage on the isotope composition ($\delta^{13}C$, $\delta^{15}N$) and nitrogen content in median leaves of grapevines. Composite leaf samples from single plants were obtained by grinding four leaves from the median part of different shoots. This process was replicated for three plants in the Chasselas (upper plots) and Pinot noir (lower plots) experimental blocks. Data are the mean ± standard error (SE) of three replicates. Different letters on the right of the symbol indicate a significant difference at $P < 0.05$ based on the Student's *t*-test. $\delta^{13}C$: Carbon isotope composition; TN: total nitrogen content; $\delta^{15}N$: nitrogen isotope composition; DI: drip irrigation; NI: no irrigation; NIP: no irrigation and plastic-covered soil.

(i.e., glycine, alanine, serine, γ-amino butyric acid, and phenylalanine) from plant tissues, and the $\delta^{15}N$ value in free proline may be higher than in bonded proline (Yoneyama and Tanaka 1999). It was recently shown for seven different vineyards of *Chardonnay* cultivar that the $\delta^{15}N$ values of the grapevine leaves were on average ~1 mUr lower than in bulk grapes and ~3.8 mUr lower than in grape proline (Paolini et al. 2016). Therefore, we believe that the reallocation of proline and probably other amino acids explain the lower leaf TN and $\delta^{15}N$ in response to water stress. It may be concluded that the interplay of biosynthesis, degradation, and extra-leaf transport processes (i.e., to grapes) of amino acids (e.g., proline) explains the observed ^{15}N depletion in leaf total nitrogen in response to water deficit. Degradation of chlorophyll (Haider et al. 2017) would release ^{15}N-rich nitrogen from the pyrrole groups, contributing to the ^{15}N-depletion in leaves of water-stressed

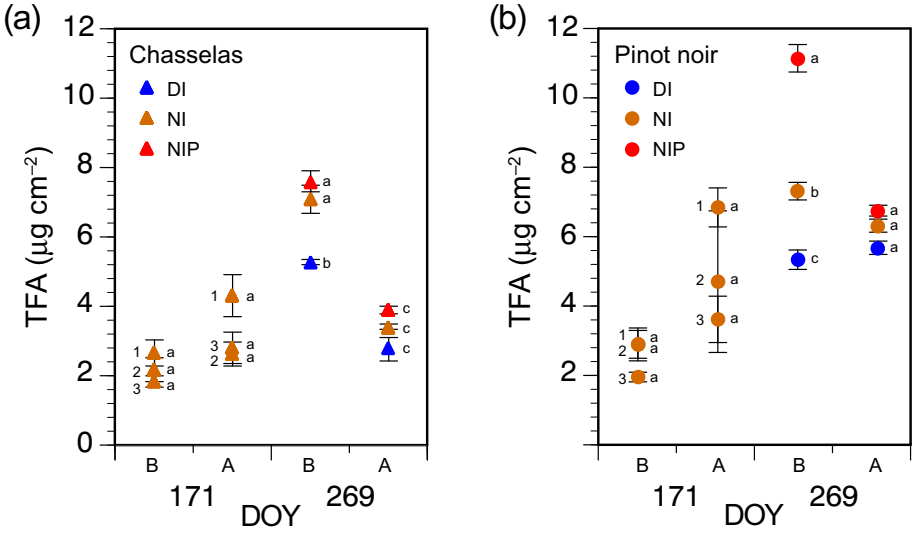

Fig. 3. Change in the total fatty acid (TFA) content of surface lipids between basal and apical leaves of grapevines at flowering and harvest. Lipids were extracted from four basal (B) and four apical (A) leaves from three plants in the Chasselas (a) and Pinot noir (b) experimental blocks. The leaves collected at flowering (DOY 171) were from three rain-fed (NI) plants, and those collected at harvest (DOY 269) were from each treatment. Data are the mean ± standard error (SE) of the replicates. Different letters indicate a significant difference between basal and apical leaves for each stage at $P < 0.05$ based on the Student's *t*-test. DI: drip irrigation; NI: no irrigation; NIP: no irrigation and plastic-covered soil.

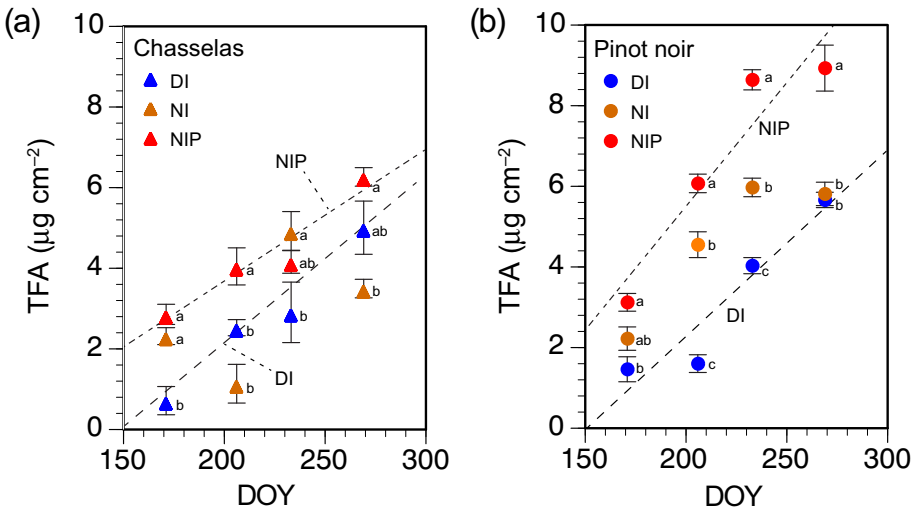

Fig. 4. Effects of water treatment and growing stage on the total fatty acids (TFAs) of the surface lipids on median leaves of grapevines. Lipids were extracted from four median leaves, each from a single plant, in the Chasselas (a) and Pinot noir (b) experimental blocks. Data are the mean ± standard error (SE) of the replicates. Different letters on the right of the symbols for each stage indicate a significant difference at $P < 0.05$ based on the Student's *t*-test. For Chasselas, the TFA-DOY regression line for well-watered (DI) vines is $y = 0.042\times - 6.45$ ($r = 0.98$, $P = 0.017$), and for water-deficient (NIP) vines, $y = 0.033\times - 2.92$ ($r = 0.96$, $P = 0.043$); for Pinot noir DI vines, $y = 0.046\times - 6.97$ ($r = 0.95$, $P = 0.053$), and for NIP vines, $y = 0.062\times - 6.86$ ($r = 0.94$, $P = 0.056$). DI: drip irrigation; NI: no irrigation; NIP: no irrigation and plastic-covered soil.

plants. Finally, carbon and nitrogen isotope analysis of bulk leaf material by EA/IMS is relatively inexpensive and fast, permitting a high throughput of samples. It is therefore an affordable approach to be integrated into a monitoring program of the soil water availability at vineyard and regional levels.

4.3. Changes in epicuticular fatty acid concentrations with leaf age and water availability

We show for both cultivars that the total FA content increased with leaf age and plant water deficit (Figs. 4 and 5). The epicuticular TFA in median leaves of both cultivars correlated negatively with Ψ_{pd}, g_s, *A*, *E* (transpiration rate), and *WUE*i, and positively with r_m (resistance), with relatively higher correlations for Pinot noir than for Chasselas (Tables 1 and 2). Thus, although plant evapotranspiration was low during the 2014 growing and the plants were under moderate to low water stress, epicuticular wax biosynthesis, secretion, and accumulation onto the cuticle surface increased in response to water deficit during the growing season. An increase in the amount of leaf cuticular lipids with water deficiency has been reported for few plants (Arabidopsis, Hegebarth et al. 2017, Kosma et al. 2009; cotton, Weete et al. 1978; tobacco, Cameron et al. 2006). The difference in the slope of the TFA-DOY regression line (Fig. 5) indicated that the accumulation of lipids on the cuticle surface occurred almost twice as fast in Pinot noir as in Chasselas vines. The Chasselas leaves, particularly the young apical leaves, demonstrated a greater fragility and thinner epidermis compared with the Pinot noir leaves, as shown by the green color of the cuticular-lipid extract produced by the release of intracellular material—mainly chlorophyll—during a short immersion of Chasselas apical leaves in organic solvents (Fig. S2). The higher rate of wax accumulation on Pinot noir leaf surfaces suggests a high environmental plasticity and adaptability of Pinot noir compared with Chasselas leaves. This result is in agreement with previous findings showing that the degree of environmental plasticity and adaptation is plant species dependent (Christophel and Gordon 2004), and that the variation in Pinot noir leaf metabolites is mainly associated with meteorological conditions (Castagna et al. 2017). This information can be very useful for breeding purposes aimed to develop grapevine varieties with high environmental adaptive capability.

The evolution of the FAs with age at the molecular level and water-deficit can be summarized for both cultivars as follows: (1) more abundant middle-chain C_{16} and C_{18} FAs on young apical leaves, with pronounced peaks for $C_{18:2}$ and $C_{18:3}$ than in old basal leaves; (2) a higher relative abundance of C_{24}–C_{32} VLCFAs in old basal leaves than young

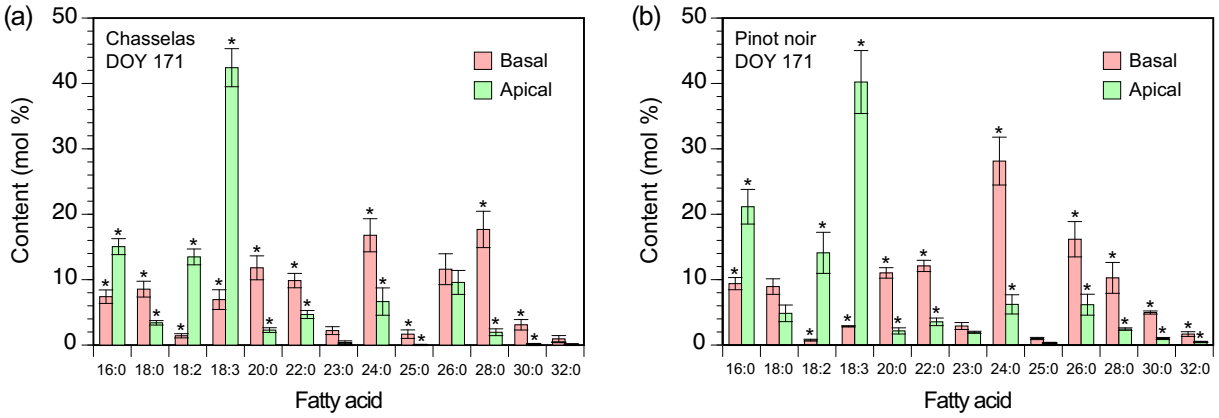

Fig. 5. Effects of age on the molar composition of fatty acids of the surface lipids on leaves from rain-fed grapevines at flowering. Basal and apical leaves of Chasselas (a) and Pinot noir (b) vines. Error bars on the columns indicate SE of the mean of four replicates. Asterisks indicate a significant difference sat $P < 0.05$ based on the Student's *t*-test.

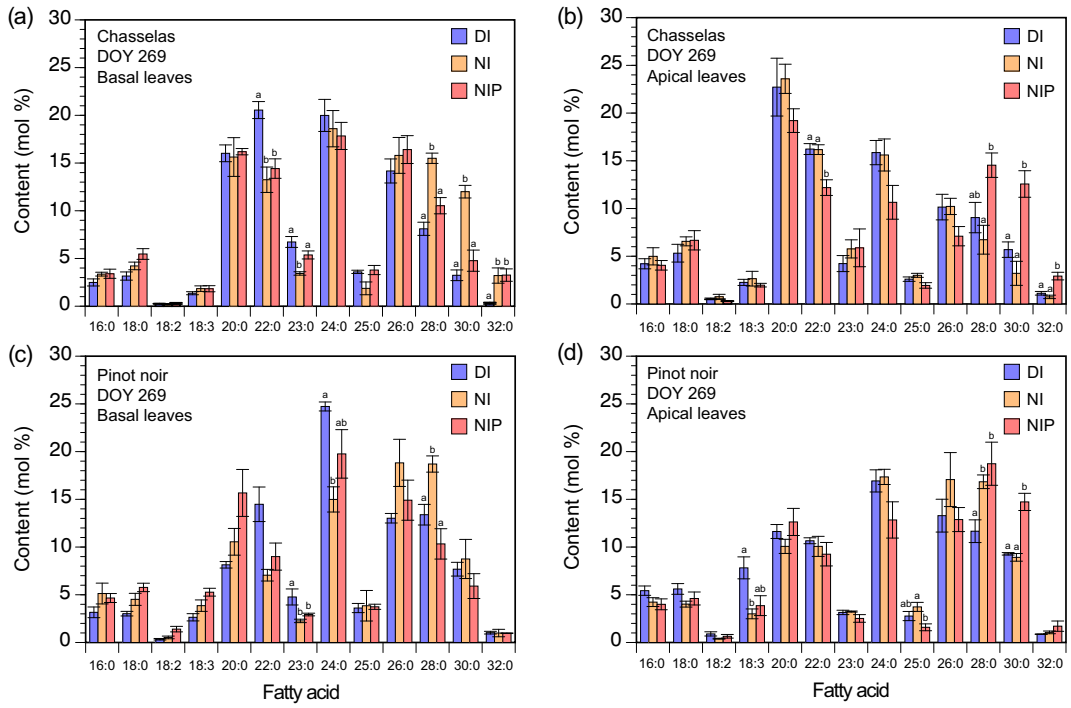

Fig. 6. Effects of age and water treatment on the molar composition of fatty acids of the surface lipids on leaves of grapevines at harvest with water treatment. Basal and apical leaves of Chasselas (upper plots), and Pinot noir (lower plots) vines. Values are the mean ± standard error (SE) of four replicates. Different letters on top of the columns for each stage indicate a significant difference at $P < 0.05$ based on the Student's *t*-test. The absence of letters in the columns for a fatty acid indicates no significant differences between treatments.

apical ones (Fig. 5, DI and NI vines in Fig. 6); and (3) significantly increased concentrations of C_{26}–C_{32} VLCFA in response to water stress compared with C>24 FAs, as shown for mature (at harvest) apical and basal leaves (Fig. 6). These trends are in line with the main biosynthetic and degradation pathways of epicuticular fatty acids. The epicuticular wax lipids are synthesized by complex, enzymatically controlled pathways and are produced and secreted by epidermal cells (Beisson et al. 2012; Kunst and Samuels 2009; Xue et al. 2017). In epidermal cells, $C_{16:0}$ and $C_{18:0}$ FAs are synthesized in the plastid and elongated in the endoplasmic reticulum (ER) to C_{20}–C_{34} VLCFAs by repeated addition of C_2 units (malonyl-CoA). The $C_{16:0}$ and $C_{18:0}$ FAs can be further desaturated both in the plastid membrane and ER to produce

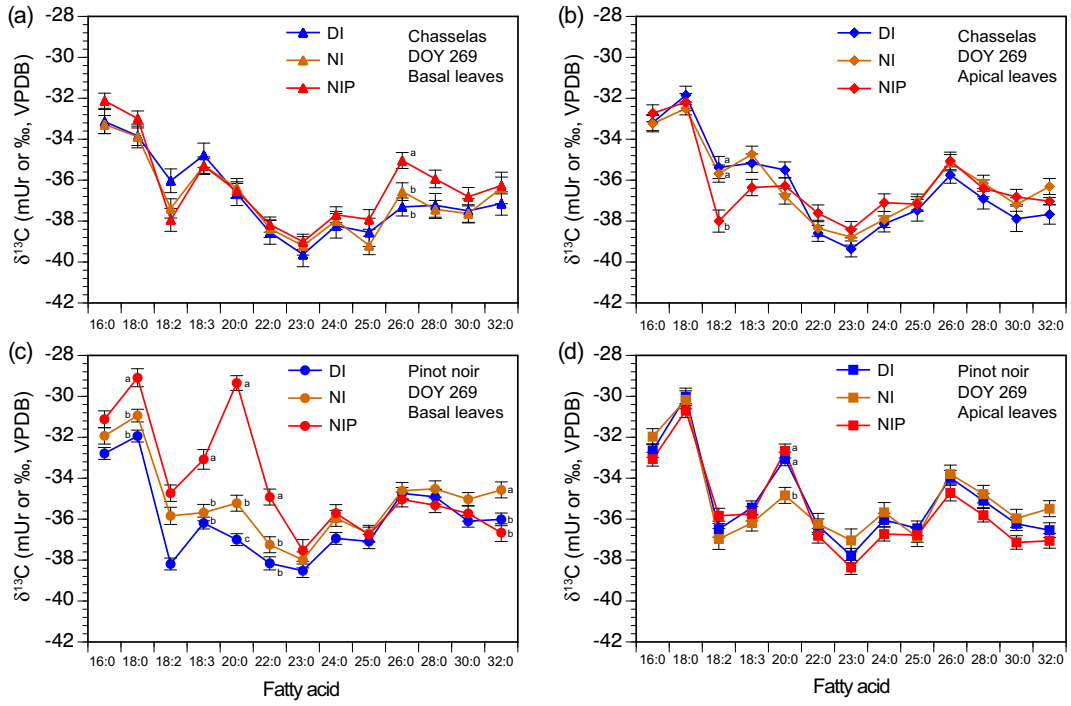

Fig. 7. Effects of age and water treatment on the carbon isotope composition ($\delta^{13}C$) of fatty acids of the surface lipids on leaves of grapevines at harvest. Values are the mean ± standard error (SE) of four replicate basal and apical leaves of Chasselas (upper plots) and Pinot noir (lower plots) vines. Different letters on the right of the symbols indicate a significant difference at $P < 0.05$ based on Student's *t*-test. The absence of letters indicates no significant differences between treatments.

Table 1
Pearson correlation correlations (r) between physiological and compositional variables of Chasselas leaves.

Variable	Ψ_{pd}	g_s	r_m	A	E	WUE_i	$\delta^{13}C$	TN	$\delta^{15}N$	TFA
Ψ_{pd}	1	0.436	−0.297	0.423	0.313	0.202	0.266	0.285	0.237	−0.508†
g_s		1	−0.965***	0.974***	0.978***	0.576*	0.376	0.779**	−0.33	−0.735**
r_m		− − − −	1	−0.974***	−0.990***	−0.690*	−0.439	−0.812**	0.431	0.654*
A		− − − −	− − − −	1	0.977***	0.743**	0.503†	0.803**	−0.367	−0.719**
E		− − − −	− − − −	+ + + +	1	0.657*	0.452	0.826***	−0.466	−0.715**
WUE_i		+ +	− −	+ + +	+ +	1	0.729**	0.624*	−0.291	−0.394
$\delta^{13}C$				+		+ + +	1	0.39	−0.284	−0.550†
TN		+ + +	− − −	+ + +	+ + +	+ +		1	−0.358	−0.407
$\delta^{15}N$									1	0.492
TFA	−	− − −	+ +	− − −	− − −		−			1

Above the diagonal (i.e., $r = 1$) the significance of the r value is denoted as *** for $P < 0.001$, ** for $P < 0.01$, * for $P < 0.05$, † for $P < 0.1$. For simplicity, bellow the diagonal (i.e., $r = 1$) + + + + or − − − − for $P < 0.001$ positive or negative correlations, + + + or − − − for $P < 0.01$, + + or − − for $P < 0.05$, + or − for $P < 0.1$. Ψ_{pd} = predawn leaf water potential; g_s = stomatal conductance; r_m = mesophyll resistance; E = transpiration; WUE_i = intrinsic water use efficiency; $\delta^{13}C$ = leaf carbon isotope composition; TN = leaf total nitrogen concentration; $\delta^{15}N$ = leaf nitrogen isotope composition; TFA = total epicuticular fatty acids concentration.

unsaturated FAs (Li et al. 2016). The VLCFAs form wax esters with primary alcohols—derived by reduction of VLCFAs—and are exported together with other components synthesized in the ER (i.e., straight-chain alcohols, aldehydes, alkanes, ketones, and free FAs) from the ER to the cuticular surface (Li et al. 2016). The observed changes in the contents of C_{16} and C_{18} FAs and the significant increase in $C_{\geq 24}$ homologs in basal compared with apical leaves indicated that FA acyl-elongation and FA turnover took place in cuticular lipids during leaf development and aging and was triggered in response to water deficit.

Additionally, the high concentrations of linoleic and linolenic acids ($C_{18:2}$ and $C_{18:3}$) in the surface lipids of young leaves (apical leaves at flowering) are explained by the release of these signaling lipids in response to wound and abiotic stress (Herde et al. 1997; Hou et al. 2016). Linolenic acid can be converted to jasmonic acid and other cyclopentanones, which are involved in the activation of plant defense against environmental stress (Okazaki and Saito 2014; Wasternack and Song 2017). The small amount of $C_{18:2}$ and $C_{18:3}$ FAs in the basal leaves for both cultivars most likely reflects the turnover of lipids during leaf senescence. Most $C_{\leq 18}$ FAs may have been either oxidized to provide energy for the senescence process or converted to mobilizable nutrients (i.e., sugars), which are relocated from mature leaves to growing younger parts of the plant (Fan et al. 2013; Xu and Shanklin 2016; Yang and Ohlrogge 2009). The most important phenomenon is that the content of total epicuticular fatty acids —a reasonable surrogate of total lipids—increases significantly in response to water deficit.

4.4. Changes in epicuticular fatty acid $\delta^{13}C$ values with water availability

We show that the precursor $C_{16:0}$ and $C_{18:0}$ FAs were significantly enriched in ^{13}C compared with the VLCFAs in all mature leaves at harvest, independently of the water treatment (Fig. 7). This phenomenon is explained by the normal growing conditions of the plant, where the vast majority of the de novo synthesized $C_{16:0}$ and $C_{18:0}$ were exported from the chloroplast to other plant tissues for the synthesis of membrane lipids (Fan et al. 2013; Yang and Ohlrogge 2009). The ^{13}C enrichment observed in most FAs (mainly in old basal leaves) with water deficiency is explained by the de novo synthesis of FAs, with successive additions of C_2 units derived from ^{13}C-rich photosynthates to produce the C_{16} and C_{18} acyl chains with relatively high $\delta^{13}C$ values in water-stressed leaves. These chains were further elongated to create $C_{>20}$ VLCFAs that were exported—if not previously reduced or decarboxylated to produce wax *n*-alcohols or *n*-alkanes— and deposited on the leaf cuticle surface, thus increasing the $\delta^{13}C$ values of the $C_{>20}$ VLCFAs accumulated in the wax lipids. In Pinot noir leaves, the highest ^{13}C enrichment due to water deficit was in the signaling $C_{18:2}$ and $C_{18:3}$ FAs and the first elongation product ($C_{20:0}$), indicating their de novo *synthesis* from ^{13}C-rich photosynthates derived from source leaves of water-stressed plants.

The observed changes in the concentrations and $\delta^{13}C$ values of leaf epicuticular FAs in Pinot noir leaves were weakly expressed in Chasselas leaves, further supporting the view that Pinot noir leaves have high plasticity and resistance to environmental changes (i.e., warming, water deficiency) (Castagna et al. 2017). Finally, the observed ^{13}C enrichment in the precursors $C_{16:0}$ and $C_{18:0}$, the VLCFAs and the bulk organic carbon in Pinot noir leaves indicate a dynamic ^{13}C discrimination through the different biosynthetic pathways between photosynthetic carbon fixation, de novo synthesis of $C_{16:0}$ and $C_{18:0}$, biosynthesis of the leaf tissues, synthesis of wax lipids, and their secretion and accumulation on the epicuticular surface. These processes seem to be relatively quick, as suggested by comparison of the corresponding $\delta^{13}C$ values of basal and apical leaves and median leaves during different phenological stages; however, the exact timing of the incorporation of newly assimilated carbon into grapevine wax lipids remains unknown. A ^{13}C-labeling study of Norway spruce showed that the incorporation of new carbon in epicuticular VLCFAs

Table 2
Pearson correlation correlations (r) between physiological and compositional variables of Pinot noir leaves.

Variable	Ψ_{pd}	g_s	r_m	A	E	WUE_i	$\delta^{13}C$	TN	$\delta^{15}N$	TFA
Ψ_{pd}	1	0.481	−0.463	0.573†	0.341	0.496	−0.196	0.373	0.243	−0.804**
g_s		1	−0.967***	0.947***	0.959***	0.224	−0.26	0.804**	−0.044	−0.727**
r_m		− − − −	1	−0.967***	−0.970***	−0.367	0.119	−0.874***	0.223	0.773**
A	+	+ + + +	− − − −	1	0.930***	0.520†	−0.076	0.858***	−0.200	−0.839***
E		+ + + +	− − − −	+ + + +	1	0.267	−0.221	0.822***	−0.211	−0.675*
WUE_i				+		1	0.442	0.407	−0.437	−0.626*
$\delta^{13}C$							1	0.133	−0.647*	0.132
TN		+ + +	− − − −	+ + + +	+ + + +			1	−0.455	−0.758**
$\delta^{15}N$							− −		1	0.08
TFA	− − −	− − −	+ + +	− − − −	− −	− −		− − −		1

Above the diagonal (i.e., $r = 1$) the significance of the r value is denoted as *** for $P < 0.001$, ** for $P < 0.01$, * for $P < 0.05$, † for $P < 0.1$. For simplicity, bellow the diagonal (i.e., $r = 1$) + + + + or − − − − for $P < 0.001$ positive or negative correlations, + + + or − − − for $P < 0.01$, + + or − − for $P < 0.05$, + or − for $P < 0.1$. Ψ_{pd} = predawn leaf water potential; g_s = stomatal conductance; r_m = mesophyll resistance; E = transpiration; WUE_i = intrinsic water use efficiency; $\delta^{13}C$ = leaf carbon isotope composition; TN = leaf total nitrogen concentration; $\delta^{15}N$ = leaf nitrogen isotope composition; TFA = total epicuticular fatty acids concentration.

occurred within 6 h of labeling and decreased with increasing chain length, being ten times lower than the precursor $C_{16:0}$ and $C_{18:0}$ FAs (Heinrich et al. 2015). Lipids may respond slowly to water deficiency-induced changes in the natural ^{13}C abundance of photosynthates, and the ^{13}C-discrimination in VLCFAs reflects a much more extended period of wax accumulation.

5. Conclusions

The results of field experiments under controlled conditions, where only the grapevine water status changed, show that the leaf $\delta^{13}C$ values in grapevines that had not received any organic foliar fertilizer (i.e., urea) increased significantly in response to soil water deficit. The total nitrogen content decreased during the growing season and generally was lower in water-stressed plants. The leaf $\delta^{15}N$ values permitted the differentiation of well-watered from water-deficient plants in both cultivars, and this phenomenon was not dependent on leaf nitrogen content and was not affected by the application of foliar urea. The total fatty acid content in epicuticular lipids was similar in the basal and apical leaves, and increased in response to water stress during the growing season. Our results suggest that leaf $\delta^{13}C$, $\delta^{15}N$, and total epicuticular FA concentrations have the potential to integrate the plant water availability over a range of time-periods (e.g., phenological stages), and they can be used as sensitive indicators of water stress even when the level of water deficit is low to moderate. In particular, the leaf $\delta^{13}C$ and $\delta^{15}N$ values can be useful as an affordable approach for biogeochemical mapping of soil water availability at the vineyard and regional scale. We believe that this finding is of relevance beyond this case study and may be applicable at the regional level to other plant species, cultivars, and growth stages. The changes in concentrations and $\delta^{13}C$ values of leaf epicuticular C_{20}-C_{24} saturated FAs and the stress-signaling linoleic and linolenic acids in Pinot noir leaves further support their high plasticity and environmental adaptive capability, which were much higher than those of Chasselas leaves. Finally, our approach combining bulk leaf $\delta^{13}C$ and $\delta^{15}N$ values, epicuticular FA concentrations, and compound-specific ^{13}C analysis improves our understanding of the dynamics of carbon and nitrogen allocation in plant leaves of different ages and plant growth stages in response to soil water availability.

Supplementary data to this article can be found online at https://doi.org/10.1016/j.scitotenv.2020.140343.

CRediT authorship contribution statement

Jorge E. Spangenberg: Conceptualization, Methodology, Data curation, Formal analysis, Visualization, Writing - original draft, Writing - review & editing.**Marc Schweizer:**Investigation, Formal analysis, Visualization.**Vivian Zufferey:**Conceptualization, Methodology, Writing - review & editing.

Declaration of competing interest

The authors declare that they have no known competing financial interests or personal relationships that could have appeared to influence the work reported in this paper.

Acknowledgments

The organic geochemistry and stable isotope facilities at the Institute of Earth Surface Dynamics have been supported by the Swiss National Science Foundation and the University of Lausanne. Assistance in preparing vineyard soil samples for stable isotope analysis was provided by Sandrine Fattore. Two anonymous reviewers are thanked for their very positive comments.

References

Bchir, A., Escalona, J.M., Galle, A., Hernandez-Montes, E., Tortosa, I., Brahama, M., Medrano, H., 2016. Carbon isotope discrimination ($\delta^{13}C$) as an indicator of vine water status and water use efficiency (WUE): looking for the most representative sample and sampling time. Agric. Water Manag. 167, 11–20.

Beisson, F., Li-Beisson, Y., Pollard, M., 2012. Solving the puzzles of cutin and suberin polymer biosynthesis. Curr. Opin. Plant Biol. 15, 329–337.

Bernard, A., Joubes, J., 2013. Arabidopsis cuticular waxes: advances in synthesis, export and regulation. Prog. Lipid Res. 52, 110–129.

Brand, W.A., 2011. New reporting guidelines for stable isotopes – an announcement to isotope users. Isot. Environ. Health Stud. 47, 535–536.

Brugnoli, E., Hubick, K.T., Voncaemmerer, S., Wong, S.C., Farquhar, G.D., 1988. Correlation between the carbon isotope discrimination in leaf starch and sugars of C_3 plants and the ratio of intercellular and atmospheric partial pressure of carbon-dioxide. Plant Physiol. 88, 1418–1424.

Cameron, K.D., Teece, M.A., Smart, L.B., 2006. Increased accumulation of cuticular wax and expression of lipid transfer protein in response to periodic drying events in leaves of tree tobacco. Plant Physiol. 140, 176–183.

Canoura, C., Kelly, M.T., Ojeda, H., 2018. Effect of irrigation and timing and type of nitrogen application on the biochemical composition of *Vitis vinifera* L. cv. Chardonnay and Syrah grapeberries. Food Chem. 241, 171–181.

Carbonneau, A., 1976. Principles and methods for measuring leaf area – attempt to define various types of leaves in Vitis genus. Annales de l'Amelioration des Plantes 26, 327–343.

Castagna, A., Csepregi, K., Neugart, S., Zipoli, G., Vecerova, K., Jakab, G., Jug, T., Llorens, L., Martinez-Abaigar, J., Martinez-Luscher, J., Nunez-Olivera, E., Ranieri, A., Schoedi-Hummel, K., Schreiner, M., Teslak, P., Tittmann, S., Urban, O., Verdaguer, D., Jensen, M.A.K., Hideg, E., 2017. Environmental plasticity of pinot noir grapevine leaves: a trans-European study of morphological and biochemical changes along a 1,500-km latitudinal climatic gradient. Plant Cell and Environment 40, 2790–2805.

Cernusak, L.A., Ubierna, N., Winter, K., Holtum, J.A.M., Marshall, J.D., Farquhar, G.D., 2013. Environmental and physiological determinants of carbon isotope discrimination in terrestrial plants. New Phytol. 200, 950–965.

Chaves, M.M., Maroco, J.P., Pereira, J.S., 2003. Understanding plant responses to drought - from genes to the whole plant. Funct. Plant Biol. 30, 239–264.

Chaves, M.M., dos Santos, T.P., Souza, C.R., Ortuño, M.F., Rodrigues, M.L., Lopes, C.M., Maroco, J.P., Pereira, J.S., 2007. Deficit irrigation in grapevine improves water-use efficiency while controlling vigour and production quality. Ann. Appl. Biol. 150, 237–252.

Christophel, D., Gordon, P., 2004. Genotypic control and environmental plasticity - foliar physiognomy and paleoecology. New Phytol. 161, 327–329.

Condon, A.G., Richards, R.A., Rebetzke, G.J., Farquhar, G.D., 2004. Breeding for high water-use efficiency. J. Exp. Bot. 55, 2447–2460.

Coplen, T.B., 2011. Guidelines and recommended terms for expression of stable-isotope-ratio and gas-ratio measurement results. Rapid Communication in Mass Spectrometry 25, 2538–2560.

Craine, J.M., Brookshire, E.N.J., Cramer, M.D., Hasselquist, N.J., Koba, K., Marin-Spiotta, E., Wang, L.X., 2015. Ecological interpretations of nitrogen isotope ratios of terrestrial plants and soils. Plant Soil 396, 1–26.

de Souza, C.R., Maroco, J.P., dos Santos, T.P., Rodrigues, M.L., Lopes, C.M., Pereira, J.S., Chaves, M.M., 2005. Impact of deficit irrigation on water use efficiency and carbon isotope composition ($\delta^{13}C$) of field-grown grapevines under Mediterranean climate. J. Exp. Bot. 56, 2163–2172.

Dominguez, E., Heredia-Guerrero, J.A., Heredia, A., 2017. The plant cuticle: old challenges, new perspectives. J. Exp. Bot. 68, 5251–5255.

Evans, R.D., 2001. Physiological mechanisms influencing plant nitrogen isotope composition. Trends Plant Sci. 6, 121–126.

Fan, J.L., Yan, C.S., Zhang, X.B., Xu, C.C., 2013. Dual role for phospholipid: diacylglycerol acyltransferase: enhancing fatty acid synthesis and diverting fatty acids from membrane lipids to triacylglycerol in Arabidopsis leaves. Plant Cell 25, 3506–3518.

Farquhar, G.D., O'Leary, M.H., Berry, J.A., 1982. On the relationship between carbon isotope discrimination and the intercellular carbon dioxide concentration in leaves. Aust. J. Plant Physiol. 9, 121–137.

Farquhar, G.D., Ehleringer, J.R., Hubick, K.T., 1989. Carbon isotope discrimination and photosynthesis. Annu. Rev. Plant Physiol. Plant Mol. Biol. 40, 503–537.

Flexas, J., Medrano, H., 2002. Drought-inhibition of photosynthesis in C_3 plants: Stomatal and non-stomatal limitations revisited. Ann. Bot. 89, 183–189.

Gaudillère, J.P., Van Leeuwen, C., Ollat, N., 2002. Carbon isotope composition of sugars in grapevine, an integrated indicator of vineyard water status. J. Exp. Bot. 53, 757–763.

Guiboileau, A., Avila-Ospina, L., Yoshimoto, K., Soulay, F., Azzopardi, M., Marmagne, A., Lothier, J., Masclaux-Daubresse, C., 2013. Physiological and metabolic consequences of autophagy deficiency for the management of nitrogen and protein resources in Arabidopsis leaves depending on nitrate availability. New Phytol. 199, 683–694.

Haider, M.S., Zhang, C., Kurjogi, M.M., Pervaiz, T., Zheng, T., Zhang, C., Lide, C., Shangguan, L., Fang, J.G., 2017. Insights into grapevine defense response against drought as revealed by biochemical, physiological and RNA-Seq analysis. Sci. Rep. 7. https://doi.org/10.1038/s41598-017-13464-3.

Handley, L.L., Austin, A.T., Robinson, D., Scrimgeour, C.M., Raven, J.A., Heaton, T.H.E., ... Stewart, G.R., 1999. The ^{15}N natural abundance ($\delta^{15}N$) of ecosystem samples reflects measures of water availability. Australian Journal of Plant Physiology 26, 185–199.

Hegebarth, D., Buschhaus, C., Joubes, J., Thoraval, D., Bird, D., Jetter, R., 2017. Arabidopsis ketoacyl-CoA synthase 16 (KCS16) forms C_{36}/C_{38} acyl precursors for leaf trichome and pavement surface wax. Plant Cell and Environment 40, 1761–1776.

Heinrich, S., Dippold, M.A., Werner, C., Wiesenberg, G.L.B., Kuzyakov, Y., Glaser, B., 2015. Allocation of freshly assimilated carbon into primary and secondary metabolites

after in situ ^{13}C pulse labelling of Norway spruce (*Picea abies*). Tree Physiol. 35, 1176–1191.
Herde, O., Pena-Cortes, H., Willmitzer, L., Fisahn, J., 1997. Stomatal responses to jasmonic acid, linolenic acid and abscisic acid in wild-type and ABA-deficient tomato plants. Plant Cell and Environment 20, 136–141.
Hobbie, E.A., Macko, S.A., Shugart, H.H., 1999. Insights into nitrogen and carbon dynamics of ectomycorrhizal and saprotrophic fungi from isotopic evidence. Oecologia 118, 353–360.
Hochberg, U., Degu, A., Cramer, G.R., Rachmilevitch, S., Fait, A., 2015. Cultivar specific metabolic changes in grapevines berry skins in relation to deficit irrigation and hydraulic behavior. Plant Physiol. Biochem. 88, 42–52.
Högberg, P., 1997. Tansley review no 95 - ^{15}N natural abundance in soil-plant systems. New Phytol. 137, 179–203.
Hou, Q.C., Ufer, G.D., Bartels, D., 2016. Lipid signaling in plant responses to abiotic stress. Plant Cell and Environment 39, 1029–1048.
Impa, S.M., Vennapusa, A.R., Bheemanahalli, R., Sabela, D., Boyle, D., Walia, H., Jagadish, S.V.K., 2020. High night temperature induced changes in grain starch metabolism alters starch, protein, and lipid accumulation in winter wheat. Plant Cell and Environment 43, 431–447.
Jefferies, R.A., MacKerron, D.K.L., 1997. Carbon isotope discrimination in irrigated and droughted potato (*Solanum tuberosum* L). Plant Cell and Environment 20, 124–130.
Jetter, R., Schaffer, S., Riederer, M., 2000. Leaf cuticular waxes are arranged in chemically and mechanically distinct layers: evidence from *Prunus laurocerasus* L. Plant Cell and Environment 23, 619–628.
Keller, M., 2005. Deficit irrigation and vine mineral nutrition. Am. J. Enol. Vitic. 56, 267–283.
Kerstiens, G., 1996. Cuticular water permeability and its physiological significance. J. Exp. Bot. 47, 1813–1832.
Kitajima, K., Mulkey, S.S., Samaniego, M., Wright, S.J., 2002. Decline of photosynthetic capacity with leaf age and position in two tropical pioneer tree species. Am. J. Bot. 89, 1925–1932.
Kosma, D.K., Bourdenx, B., Bernard, A., Parsons, E.P., Lu, S., Joubes, J., Jenks, M.A., 2009. The impact of water deficiency on leaf cuticle lipids of Arabidopsis. Plant Physiol. 151, 1918–1929.
Kunst, L., Samuels, L., 2009. Plant cuticles shine: advances in wax biosynthesis and export. Curr. Opin. Plant Biol. 12, 721–727.
Lawlor, D.W., Cornic, G., 2002. Photosynthetic carbon assimilation and associated metabolism in relation to water deficits in higher plants. Plant Cell and Environment 2, 275–294.
Li, N.N., Xu, C.C., Li-Beisson, Y.H., Philippar, K., 2016. Fatty acid and lipid transport in plant cells. Trends Plant Sci. 21, 145–158.
Liu, Z., Zhang, Y.Z., Zhang, Y., Yang, G.L., Shao, S.Z., Nie, J., Yuan, Y.W., Rogers, K.M., 2019. Influence of leaf age, species and soil depth on the authenticity and geographical origin assignment of green tea. Rapid Commun. Mass Spectrom. 33, 625–634.
Mundim, F.M., Pringle, E.G., 2018. Whole-plant metabolic allocation under water stress. Front. Plant Sci. 9. https://doi.org/10.3389/fpls.2018.00852.
Okazaki, Y., Saito, K., 2014. Roles of lipids as signaling molecules and mitigators during stress response in plants. Plant J. 79, 584–596.
Paolini, M., Ziller, L., Bertoldi, D., Bontempo, L., Larcher, R., Nicolini, G., Camin, F., 2016. $\delta^{15}N$ from soil to wine in bulk samples and proline. J. Mass Spectrom. 51, 668–674.
Peuke, A.D., Gessler, A., Tcherkez, G., 2013. Experimental evidence for diel $\delta^{15}N$ -patterns in different tissues, xylem and phloem saps of castor bean (Ricinus communis L.). Plant Cell and Environment 36, 2219–2228.
Robinson, D., Handley, L.L., Scrimgeour, C.M., Gordon, D.C., Forster, B.P., Ellis, R.P., 2000. Using stable isotope natural abundances ($\delta^{15}N$ and $\delta^{13}C$) to integrate the stress responses of wild barley (*Hordeum spontaneum* C. Koch.) genotypes. J. Exp. Bot. 51, 41–50.
Schimmelmann, A., Qi, H. P., Coplen, T. B., Brand, W. A., Fong, J., Meier-Augenstein, W., Kemp, H. F., Toman, B., Ackermann, A., Assonov, S., Aerts-Bijma, A. I., Brechcha, R., Chikaraishi, Y., Daewish, T., Elsner, M., Gehre, M., Geilmann, H., Groing, M., Helie, J. F., Herrero-Martin, S., Meijer, H. A. J., Sauer, P. E., Sessions, Werner, R. A. 2016. Organic reference materials for hydrogen, carbon, and nitrogen stable isotope-ratio measurements: caffeines, *n*-alkanes, fatty acid methyl esters, glycines, L-valines, polyethylenes, and oils. Anal. Chem., 88, 4294–4302.
Schultz, H.R., Kiefer, W., Gruppe, W., 1996. Photosynthetic duration, carboxylation efficiency and stomatal limitation of sun and shade leaves of different ages in field-grown grapevine (Vitis vinifera L.). Vitis 35, 169–176.
Serret, M.D., Yousfi, S., Vicente, R., Pinero, M.C., Otalora-Alcon, G., del Amor, F.M., Araus, J.L., 2018. Interactive effects of CO_2 concentration and water regime on stable isotope signatures, nitrogen assimilation and growth in sweet pepper. Front. Plant Sci. 8. https://doi.org/10.3389/fpls.2017.02180.
Spangenberg, J.E., Zufferey, V., 2018. Changes in soil water availability in vineyards can be traced by the carbon and nitrogen isotope composition of dried wines. Sci. Total Environ. 635, 178–187.
Spangenberg, J.E., Zufferey, V., 2019. Carbon isotope compositions of whole wine, wine solid residue, and wine ethanol, determined by EA/IRMS and GC/C/IRMS, can record the vine water status-a comparative reappraisal. Anal. Bioanal. Chem. 41, 2031–2043.
Spangenberg, J.E., Ferrer, M., Jacomet, S., Bleicher, N., Schibler, J., 2014. Molecular and isotopic characterization of lipids staining bone and antler tools in the late Neolithic settlement, Zurich opera parking, Switzerland. Org. Geochem. 69, 11–25.
Spangenberg, J.E., Vogiatzaki, M., Zufferey, V., 2017. Gas chromatography and isotope ratio mass spectrometry of pinot noir wine volatile compounds ($\delta^{13}C$) and solid residues ($\delta^{13}C$, $\delta^{15}N$) for the reassessment of vineyard water-status. J. Chromatogr. A 1517, 142–155.
Srivastava, K., Wiesenberg, G.L.B., 2018. Severe drought-influenced composition and $\delta^{13}C$ of plant and soil *n*-alkanes in model temperate grassland and heathland ecosystems. Org. Geochem. 116, 77–89.
Stines, A.P., Naylor, D.J., Hoj, P.B., van Heeswijck, R., 1999. Proline accumulation in developing grapevine fruit occurs independently of changes in the levels of Δ^1-pyrroline-5-carboxylate synthetase mRNA or protein. Plant Physiol. 120, 923–931.
Stock, W.D., Evans, J.R., 2006. Effects of water availability, nitrogen supply and atmospheric CO_2 concentrations on plant nitrogen natural abundance values. Funct. Plant Biol. 33, 219–227.
Tcherkez, G., Hodges, M., 2008. How stable isotopes may help to elucidate primary nitrogen metabolism and its interaction with (photo)respiration in C_3 leaves. J. Exp. Bot. 58, 1685–1693.
Tegeder, M., Masclaux-Daubresse, C., 2018. Source and sink mechanisms of nitrogen transport and use. New Phytol. 217, 35–53.
van Leeuwen, C., Tregoat, O., Chone, X., Bois, B., Pernet, D., Gaudillere, J.P., 2009. Vine water status is a key factor in grape ripening and vintage quality for red Bordeaux wine. How can it be assessed for vineyard management purposes? Journal International des Sciences de da Vigne et du Vin 43, 121–134.
Wang, J., Xu, Y.P., Zhou, L.P., Shi, M.R., Axia, E., Jia, Y.F., Chen, Z.X., Li, J.Z., Wang, G.A., 2018. Disentangling temperature effects on leaf wax n-alkane traits and carbon isotopic composition from phylogeny and precipitation. Org. Geochem. 126, 13–22.
Wasternack, C., Song, S.S., 2017. Jasmonates: biosynthesis, metabolism, and signaling by proteins activating and repressing transcription. J. Exp. Bot. 68, 1303–1321.
Weete, J.D., Leek, G.L., Peterson, C.M., Currie, H.E., Branch, W.D., 1978. Lipid and surface wax synthesis in water-stressed cotton leaves. Plant Physiol. 62, 675–677.
Werner, R.A., Schmidt, H.L., 2002. The in vivo nitrogen isotope discrimination among organic plant compounds. Phytochemistry 61, 465–484.
Werth, M., Mehltreter, K., Briones, O., Kazda, M., 2015. Stable carbon and nitrogen isotope compositions change with leaf age in two mangrove ferns. Flora 210, 80–86.
Wu, M.S., Feakins, S.J., Martin, R.E., Shenkin, A., Bentley, L.P., Blonder, B., Salinas, N., Asner, G.P., Malhi, Y., 2017. Altitude effect on leaf wax carbon isotopic composition in humid tropical forests. Geochim. Cosmochim. Acta 206, 1–17.
Xu, C.C., Shanklin, J., 2016. Triacylglycerol metabolism, function, and accumulation in plant vegetative tissues. In: Merchant, S.S. (Ed.), Annual Review of Plant Biology. 67, pp. 179–206.
Xue, D.W., Zhang, X.Q., Lu, X.L., Chen, G., Chen, Z.H., 2017. Molecular and evolutionary mechanisms of cuticular wax for plant drought tolerance. Front. Plant Sci. 8. https://doi.org/10.3389/fpls.2017.00621.
Yang, Z.L., Ohlrogge, J.B., 2009. Turnover of fatty acids during natural senescence of Arabidopsis, *Brachypodium*, and switchgrass and in Arabidopsis β-oxidation mutants. Plant Physiol. 150, 1981–1989.
Yoneyama, T., Tanaka, F., 1999. Natural abundance of ^{15}N in nitrate, ureides, and amino acids from plant tissues. Soil Science and Plant Nutrition 45, 751–755.
Yousfi, S., Serret, M.D., Araus, J.L., 2009. Shoot $\delta^{15}N$ gives a better indication than ion concentration or $\delta^{13}C$ of genotypic differences in the response of durum wheat to salinity. Funct. Plant Biol. 36, 144–155.
Yousfi, S., Serret, M.D., Marquez, A.J., Voltas, J., Araus, J.L., 2012. Combined use of $\delta^{13}C$, $\delta^{18}O$ and $\delta^{15}N$ tracks nitrogen metabolism and genotypic adaptation of durum wheat to salinity and water deficit. New Phytol. 194, 230–244.
Zinta, G., AbdElgawad, H., Peshev, D., Weedon, J.T., Van den Ende, W., Nijs, I., Janssens, I.A., Beemster, G.T.S., Asard, H., 2018. Dynamics of metabolic responses to periods of combined heat and drought in *Arabidopsis thaliana* under ambient and elevated atmospheric CO_2. J. Exp. Bot. 69, 2159–2170.
Zufferey, V., Murisier, F., Schultz, H.R., 2000. A model analysis of the photosynthetic response of *Vitis vinifera* L. cvs Riesling and Chasselas leaves in the field: I. interaction of age, light and temperature. Vitis 39, 19–26.
Zufferey, V., Spring, J.L., Verdenal, T., Dienes, A., Belcher, S., Lorenzini, F., Koestel, C., Rösti, J., Gindro, K., Spangenberg, J., Viret, O., 2017. Influence of water stress on plant hydraulics, gas exchange, berry composition and quality of pinot noir wines in Switzerland. Oeno One 51, 37–57.
Zufferey, V., Verdenal, T., Dienes, A., Belcher, S., Lorenzini, F., Koestel, C., Rösti, J., Gindro, K., Spangenberg, J.E., Viret, O., Spring, J.L., 2018. The impact of plant water status on the gas exchange, berry composition and wine quality of Chasselas grapes in Switzerland. Oeno One 52, 347–361.